Journal of Applied Polymer Science

Shape-memory behavior of high-strength amorphous thermoplastic poly(*para*-phenylene)

David A. Collins,[1] Christopher M. Yakacki,[2] Daniel Lightbody,[2] Ravi R. Patel,[2] Carl P. Frick[1]
[1]Department of Mechanical Engineering, University of Wyoming, Laramie, Wyoming
[2]Department of Mechanical Engineering, University of Colorado Denver, Denver, Colorado
Correspondence to: C. P. Frick (E-mail address: cfrick@uwyo.edu)

ABSTRACT: The purpose of this study was to investigate the shape-memory behavior of poly(*para*-phenylene) (PPP) under varying programming temperatures, relaxation times, and recovery conditions. PPP is an inherently stiff and strong aromatic thermoplastic, not previously investigated for use as a shape-memory material. Initial characterization of PPP focused on the storage and relaxation moduli for PPP at various frequencies and temperatures, which were used to develop continuous master curves for PPP using time–temperature superposition (TTS). Shape-memory testing involved programming PPP samples to 50% tensile strain at temperatures ranging from 155°C to 205°C, with varying relaxation holds times before cooling and storage. Shape-recovery behavior ranged from nearly complete deformation recovery to poor recovery, depending heavily on the thermal and temporal conditions during programming. Straining for extended relaxation times and elevated temperatures significantly decreased the recoverable deformation in PPP during shape-memory recovery. However, PPP was shown to have nearly identical full recovery profiles when programmed with decreased and equivalent relaxation times, illustrating the application of TTS in programming of the shape-memory effect in PPP. The decreased shape recovery at extended relaxation times was attributed to time-dependent visco-plastic effects in the polymer becoming significant at longer time-scales associated with the melt/flow regime of the master curve. Under constrained-recovery, recoverable deformation in PPP was observed to have an exponentially decreasing relationship to the bias stress. This study demonstrated the effective use of PPP as a shape-memory polymer (SMP) both in mechanical behavior as well as in application. © 2015 Wiley Periodicals, Inc. J. Appl. Polym. Sci. **2016**, *133*, 42903.

KEYWORDS: mechanical properties; properties and characterization; structure–property relations; thermoplastics

Received 21 June 2015; accepted 2 September 2015
DOI: 10.1002/app.42903

INTRODUCTION

Shape-memory polymers (SMPs) are a class of smart materials that have the ability to "memorize" a permanent shape, maintain a temporary shape after deformation, and return to the permanent shape upon the application of external stimulation – for SMP recent reviews see Refs. 1–10. Relative to other shape-memory materials, SMPs have many desirable properties, including high recoverable strains, low cost, tunable properties, biocompatibility, degradability, and ease of processing. These properties make SMPs useful for a wide variety of applications, such as biomedical devices,[11–13] actuators in flexible electronics,[14,15] and 4D printed materials.[16,17]

The majority of SMPs are triggered via thermal actuation, such that heat is the stimulus used to induce recovery and can be provided by conduction, convection, photo-thermal effects, inductive heating, or resistive heating. A typical thermal-based shape-memory cycle[18,19] consists of deforming the material in the vicinity of a transition temperature inherent to the material, either a glass or melting transition. While the strain is maintained, the material is cooled sufficiently below this transition temperature to "freeze" the material in the desired deformed shape. Molecular chain motion and recovery is restricted via the formation of crystalline regions in semi-crystalline SMPs or the reduction in free volume and micro-Brownian motion in amorphous SMPs. Recovery is induced by heating the sample near or above the transition temperature, at which point the sample returns to its original state. Recovery is enabled by an increase in chain mobility associated with the transition temperature and is driven by entropy elasticity. It is necessary for SMPs to be crosslinked, either chemically or physically, for the material to "remember" its original configuration.

Despite their advantages, the inherent low strength and stiffness of SMPs can limit possible applications. A common method to improve polymer strength and stiffness is to increase the chemical crosslinking, or the addition of reinforcement such as glass/carbon fibers; however, both approaches severely limit ductility,

effectively negating the purpose of an SMP. Aromatic polymers, such as poly(phenylene sulfide) (PPS) and poly(ether etherketone) (PEEK), are unique and advantageous because they are stronger and stiffer than more common polymers and have large fracture strains relative to composites.[20–24] The defining microstructural feature of these materials is the abundance of phenyl rings in the polymer backbone, which results in high strength, high stiffness, and stability at high temperatures. However, relatively few aromatic polymers have been explored for use as SMPs. This is in part due to the lack of physical or chemical crosslinks in aromatic thermoplastics typically needed to help the polymer remember its original shape.[25] Therefore, researchers have added such features to aromatic polymers to improve shape memory behavior via modified chain structures,[26] the addition of modified graphene,[27] or light covalent crosslinking plus the addition carbon nanotubes.[28] Nonetheless, shape memory investigation of neat polymide[27] and PEEK[29,30] demonstrated reasonable shape fixity and deformation recovery.

In addition to well-known PPS and PEEK materials, poly(*para*-phenylene) (PPP) is an aromatic polymer consisting of a directly linked phenyl backbone. Various types of PPP with different side groups have been investigated as structural materials, and modulus values ranging from 5 GPa to 9 GPa and tensile strengths ranging from 120 MPa to 200 MPa have been reported.[31–35] PPP is an amorphous thermoplastic, and can be formed by extrusion,[36] hot compression molding,[31] injection molding,[37] or solution casting.[38] Since PPP is amorphous it does not require prescribed cooling rates or subsequent heat treatments to achieve the desired properties, which are often required for increasing crystalline volume fraction in polymers like PEEK.[39–42]

The purpose of this study is to investigate the shape-memory behavior of PPP. Although PPP is an amorphous thermoplastic, and therefore does not contain chemical crosslinks or crystalline segments typically considered prerequisites for good shape-recovery behavior, the results presented here demonstrate that the relatively stiff molecular structure of PPP leads to stable entanglements, which effectively act as the "hard points" necessary to drive shape recovery. However, the inherent nature of PPP will make its shape-memory behavior sensitive to viscous effects and time/temperature dependent properties near or above the glass transition. Therefore, the principle of time–temperature superposition (TTS) was used to understand and predict how the programming conditions (i.e. time and temperature) affect the recovery behavior. TTS asserts that for a thermorheologically simple material, a change in temperature will have the same effect on the viscoelastic properties as a corresponding change in time and those equivalent time–temperature changes can be related through a simple, empirically-derived equation. Although other amorphous thermoplastics have shown shape-memory behavior,[25] researchers have not yet investigated an experimental correlation between TTS and shape recovery in these materials.

In this study, the thermomechanical properties of PPP were evaluated using dynamic mechanical analysis to determine the glass transition characteristics of the material, establish its thermorheological simplicity, and construct its master curves. The tensile properties of PPP were characterized at various temperatures, confirming that PPP has appropriate ductility necessary for practical shape-memory applications. Free-recovery shape-memory tests were performed to establish the qualitative effects of changes in temperature and/or deformation time during programming, and constrained recovery tests were performed to determine the work capacity of the material during recovery. Additional free-recovery tests were performed to confirm that the recovery behavior of PPP could be predicted using TTS.

EXPERIMENTAL

Material and Compression Molding

PPP (PrimoSpire® PR-250) was provided by Solvay Specialty Polymers, LLC (Alpharetta, GA). The material was used in its as-received condition. Previous studies have investigated the structure and mechanical properties of PR-250 in ambient conditions,[31,43–45] although elevated temperature testing has not previously been reported. For this type of PPP at room temperature, the modulus is 5 GPa–5.5 GPa, the tensile yield strength is 141 MPa–149 MPa, the tensile fracture strength is 120 MPa–127 MPa, and the strain-to-failure is 16%–17%.

Flat plate samples were formed by compression molding PPP powder using a hydraulic high-temperature press (Model DV-62-422, Pasadena Hydraulics, City of Industry, CA). Approximately, 15 cm^3 of PPP powder was pressed between two aluminum platens wrapped in non-stick aluminum foil. This mold was pressed under 1,334 N at 250°C for 10 min. The mold was removed from the press and allowed to air cool for 10 min. The resulting product was a solid PPP disk roughly 10 cm in diameter and 0.5 mm–0.9 mm thick. Several disks were manufactured as needed.

Dynamic Mechanical Analysis

Dynamic mechanical analysis (DMA) was performed using a dynamic mechanical analyzer (Q800, TA Instruments, New Castle, DE). A rectangular strip was cut from a PPP disk with a rotary abrasive disk and its edges were sanded with 220 grit sandpaper to smooth surface imperfections or rough edges. The strip was 35 mm long, 5 mm wide, and 0.5 mm thick. The strip was installed in the tensile clamps of the DMA using 791 Nmm of torque at both clamps. The gauge length of the sample was approximately 22 mm. The sample was thermally equilibrated to 130°C and allowed to saturate for 10 min. The sample was then heated to 230°C at 1°C/min while subjected to a dynamic strain of 0.1% at a frequency of 1 Hz. The force track was set to 125%. The transition onset temperature, T_{onset}, was defined as the intersection of the lines tangent to the storage modulus curve at 130°C and its inflection point in the transition regime (~176°C), while the glass transition temperature, T_g, was defined at the peak of the tan δ curve.

Samples used to form the storage modulus master curve were subjected to a dynamic strain of 0.1% at frequencies of 0.46, 1, 2.15, 4.64, 10, 21.54, and 46.42 Hz at temperatures ranging from 155°C to 205°C in 5°C increments. The temperature was held isothermally for 10 min at each increment. Four duplicate samples were tested to ensure repeatability. To generate the master curve, the frequency-dependent storage modulus component

curves for each test temperature were plotted together on a semi-log scale. Using 185°C as the reference temperature, T_{ref}, the frequencies for each component curve were shifted by the appropriate value until each component curve superposed those nearest it, forming a continuous curve. The value used for the shift in frequency for the set of data corresponding to each temperature is typically referred to as the shift factor (a_T).

The relaxation modulus master curve was created using data from samples deformed quasi-instantaneously to 0.25% strain and allowed to relax for 20 min at temperatures ranging from 155°C to 205°C in 5°C increments. Four duplicate samples were tested to confirm repeatability. Once the time-dependent relaxation modulus component curves had been established for each temperature, the relaxation modulus master curve was generated using an analogous procedure as the storage modulus master curve.

It is important to note that the relaxation modulus tests were performed under static conditions and measured stress relaxation as a function of time, whereas the storage modulus tests were performed under dynamic conditions and measure the amounts of stored and lost energy. For thermorheologically simple materials, both tests should yield similar Williams–Landel–Ferry (WLF) constants. For this study, the storage modulus tests were particularly useful for identifying T_g and modulus values at specific temperatures, while the relaxation modulus master curve was useful to identifying the melt/flow regime as a function of time.

WLF Constants

Williams *et al.*[46] proposed that for a polymer with a single relaxation mechanism, the temperature dependence is related through the equation:

$$\log(a_T) = -\frac{c_1(T - T_{ref})}{c_2 + T - T_{ref}} \quad (1)$$

where a_T is the shift factor for temperature T, T_{ref} is the reference temperature, and c_1 and c_2 are empirically-derived constants, known as the WLF constants. For the analysis shown here, $T_{ref} = 185$°C.

Equation (1) can be rearranged as:

$$T - T_{ref} = -\frac{c_1(T - T_{ref})}{log(a_T)} - c_2. \quad (2)$$

Examining the data on a $(T–T_{ref})$ vs $(T–T_{ref})/\log(a_T)$ plot revealed a linear curve whose slope is $–c_1$ and whose y-intercept is $–c_2$. It should be noted that the shift factors for the 155°C component curves (the uppermost component curve for both storage and relaxation modulus) were not used to calculate the WLF constants. An equivalent approach was used to calculate the shift factors for the relaxation modulus master curve, except the corresponding regression curve will have a positive slope.

Tensile Strain-to-Failure Testing

Dog bone samples were cut from the PPP disks using a routing template. The edges were sanded to remove any surface flaws prior to testing. The gauge sections were about 0.6 to 0.9 mm thick, 3.02 to 3.25 mm wide, and 15.8 to 28.4 mm long. The tensile tests were performed using a mechanical load frame (Insight 30, MTS, Eden Prairie, MN) equipped with a laser extensometer (LX 500, MTS) and thermal chamber (Therm-Craft, Winston-Salem, NC). The gauge sections of the samples were marked with reflective tape and the samples were secured to the top grip of the load frame. The samples were heated to the test temperature and allowed to saturate for 10 min before the thermal chamber was opened and the sample was secured to the bottom grip. The chamber was re-saturated to the test temperature and the samples were deformed at 0.1 mm/s until failure. Samples were tested at 155, 175, 195, and 205°C. Several samples were tested at each temperature to ensure repeatability.

Shape-Memory Testing

Shape-memory tests were performed in a similar manner to tensile testing, using the same equipment. Samples were deformed to 50% strain at a specified temperature. Upon reaching 50% strain, the thermal chamber was immediately purged with liquid nitrogen until the temperature in the chamber reached 100°C. This temperature was maintained for 10 min before the sample was unloaded. The fixity ratio (R_f) of the samples was defined by:

$$R_f = \frac{\varepsilon_{unload}}{\varepsilon_{\max}} \quad (3)$$

where ε_{max} is the maximum strain during programming and ε_{unload} is the strain after the sample was unloaded. Duplicate samples were programmed at each temperature.

To initiate free recovery, the samples were secured only to the top grip of the load frame. The thermal chamber was equilibrated at 100°C for at least 10 min before testing began. Recovery was induced by heating the thermal chamber at 3°C/min to 230°C. The maximum recovery ratio (R_r) was defined by the equation:

$$R_r = \frac{\varepsilon_{initial} - \varepsilon_{final}}{\varepsilon_{initial}} \quad (4)$$

where $\varepsilon_{initial}$ is the strain at the beginning of the recovery segment when the sample is unloaded, and ε_{final} is the strain at the end of the recovery segment. The recovery ratio was also calculated as a function of temperature by replacing ε_{final} with the strain measurement at a specific temperature, $\varepsilon(T)$.

$$R_r(T) = \frac{\varepsilon_{initial} - \varepsilon(T)}{\varepsilon_{initial}} \quad (5)$$

It should be noted that fixity and recovery ratios are often multiplied by 100 to give fixity and recovery values in percentages. The rate of recovery was determined by the slope of the R_r curve as a function of temperature. For a given recovery curve, the recovery initiation temperature (T_i) was defined as the temperature at the intersection of two tangent lines, where the lines were set at the beginning of the curve and when half of the stored strain was recovered. A representative free-recovery test programmed at 175°C as a function of time is shown in Figure 1.

The procedure for shape-memory testing with relaxation time was similar to the procedure for the previous set of shape memory tests, except once the samples had reached 50% strain they

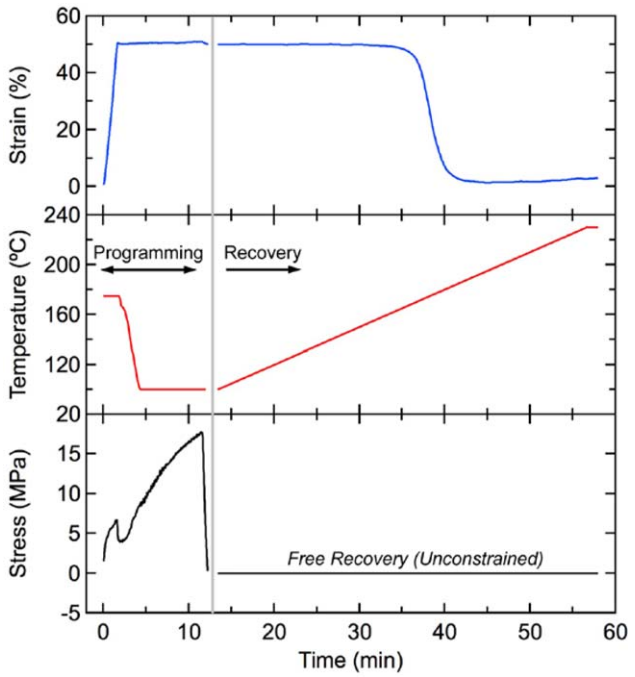

Figure 1. Representative free-recovery (unconstrained) shape-memory cycle illustrating programming and deformation recovery as a function of time. Deformation temperature was 175°C. [Color figure can be viewed in the online issue, which is available at wileyonlinelibrary.com.]

were allowed to relax for 100 min. For some samples, the gauge section tended to contract during relaxation. To counteract this, every 10 min the sample was quickly deformed back to 50% strain. After relaxation, the sample was immediately cooled to room temperature. After maintaining this temperature for 10 min, the load on the sample was removed. The programming temperatures were 175°C, 195°C, and 205°C. The procedure for the recovery segment was the same as for the samples with no relaxation time.

Partially constrained recovery tests were performed using the DMA machine. The samples were allowed to equilibrate at 175°C, then loaded in tension at a rate of 5.5 to 12 MPa per minute for 1 min to reach approximately 50% strain. The samples were quickly cooled to 100°C and maintained at this temperature for 5 min. The samples were then heated at 3°C per minute to 230°C under a constant bias stress ranging from 0 MPa to 8.9 MPa. Repeat samples were tested at each constraining load.

Shape-Memory Demonstration

The explicit purpose of this testing was to uniformly deform a hollow PPP tube to demonstrate shape-memory behavior. PPP tubes were machined from an extruded solid rod to a length of 20 mm, with an inner diameter of 8 mm and outer diameter of 9.6 mm. Sixteen stainless steel wires, 1.15 mm in diameter, were arranged in a circular pattern within the tube and held in place using a custom fixture. The fixture was heated to a temperature of 175°C and allowed to equilibrate for 10 min. Following equilibration, a 10.7 mm steel plunger was pushed through the center of the wires at a rate of 0.02 mm/sec. Approximately, 10 min after the insertion began, the plunger was fully inserted through the center of the expanded PPP tube. The fixture was then removed from the thermal chamber and quenched in water to rapidly cool the polymer. The maximum expanded diameter for the tube was 13 mm. The R_f and R_r were calculated using the change in circumference of the tube after expansion. The samples then underwent recovery at 200°C for 10 min.

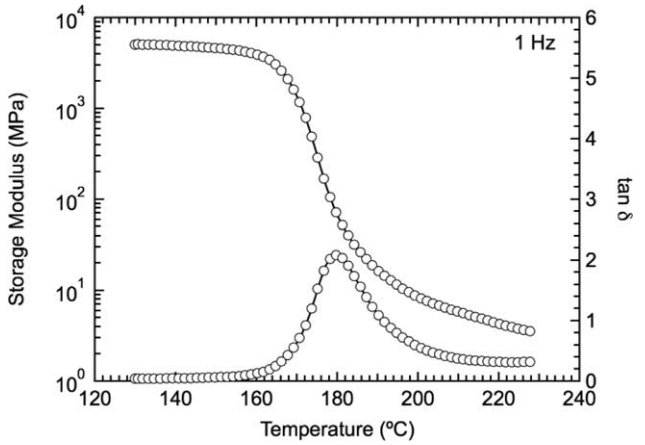

Figure 2. Representative storage modulus and tan δ curves for PPP. The glass transition temperature is defined as the peak of the tan δ curve, approximately 180°C.

RESULTS

Dynamic Mechanical Analysis

The storage modulus and tan δ measurements of PPP as a function of temperature are shown in Figure 2. The storage modulus curve took on the expected shape for an amorphous thermoplastic. At low temperatures, the storage modulus was observed to be relatively high, approximately 5 GPa. It decreased steadily with temperature until approximately 165°C, when it decreased by approximately two decades over a 20°C span. The rate of change in the storage modulus decreased after about 185°C, but it continued to decrease steadily as the temperature increased. The T_{onset} and T_g of PPP were measured at 167°C and 180°C, respectively.

Master curves developed using storage modulus and relaxation modulus data are shown in Figure 3(a,b), respectively. In general, both curves were constructed using the same approach. Measurements were taken at seven discrete frequencies under isothermal conditions, resulting in the 10 data sets labeled as component curves in Figure 3. Each data set was then shifted relative to a reference temperature, chosen to be $T_{ref} = 185$°C, such that a continuous curve, or master curve, is formed. The general shapes of both master curves are consistent with amorphous thermoplastics in the vicinity of the glass transition. The storage modulus data begins at relatively low values of approximately 5 MPa at 0.01 Hz, enters a transition zone from 0.1 Hz to 1000 Hz, and plateaus at 3.5 GPa by 10,000 Hz. Conversely, the relaxation modulus shows an expected inverse relationship; values of approximately 1 GPa are observed at 0.001 sec, a transition zone from 0.01 sec to 10 sec, and then a plateau region ranging from 6 MPa to 3 MPa. A notable difference between

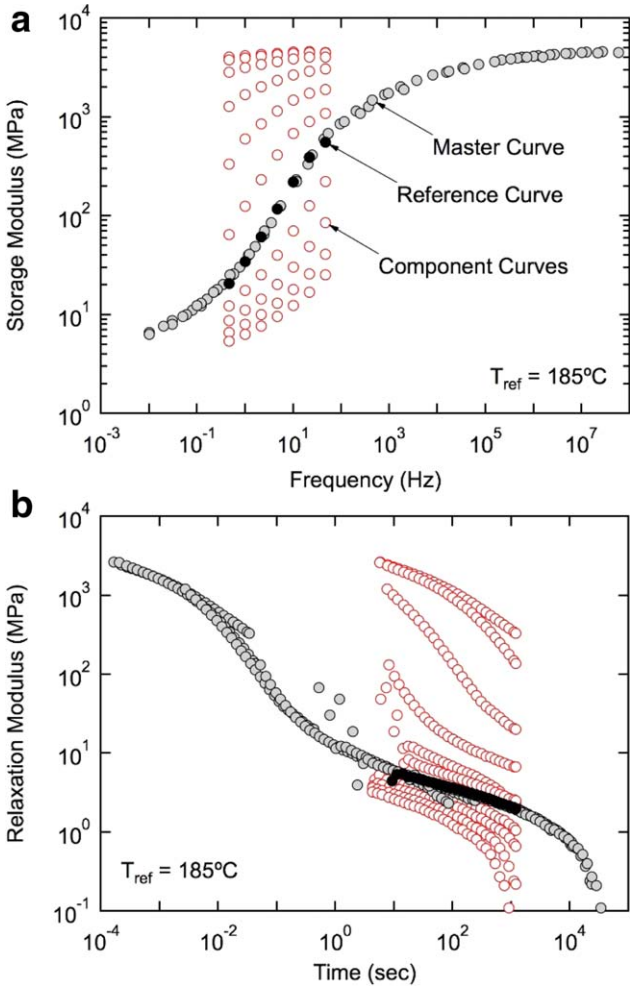

Figure 3. PPP Component, reference, and master curves for the (a) storage modulus and (b) relaxation modulus. The reference temperature is 185°C, and the component curves vary in temperature from 155°C to 205°C in 5°C increments. [Color figure can be viewed in the online issue, which is available at wileyonlinelibrary.com.]

the storage modulus and the relaxation modulus master curves is that the latter better captures the flow regime of the PPP material at increased times and temperatures, marked by the distinct drop in relaxation modulus at 10,000 sec.

For the relaxation modulus shown in Figure 3(b), it is necessary to note that some individual data points that stood apart from the master curve in the vicinity of 1 sec. The curves in this region represented data recorded near T_g, where the viscoelastic and damping properties of the material are relatively high. Close observation of the data reveal that the relaxation modulus curve tended to oscillate initially before settling into a smooth decay. Despite this, the steady-state regions of the component curves fell along the master curve, indicating that the transient response of the material to an input did not affect its steady-state response.

The WLF constants calculated independently for each storage and relaxation modulus master curve were determined by fitting a linear curve to each set of data points in accordance with eq. (2), as shown in Table I. Overall, there is good agreement between the two approaches with the ranges of each constant overlapping. The average WLF constants for the storage modulus were $C_1 = 6.83$ and $C_2 = 51.6$ K; for the relaxation modulus the averages were $C_1 = 6.00$ and $C_2 = 54.8$ K.

Table I. WLF Constants Described by eq. (2) Calculated Independently Using Data from the Storage and Relaxation Modulus Master Curves (T_{ref} = 185°C)

	C_1	C_2 (K)
Storage modulus	6.40–7.27	48.9–54.3
Relaxation modulus	5.74–6.24	52.0–59.8

Stress–Strain Behavior

Representative strain-to-failure curves as a function of temperature are shown in Figure 4. At 155°C, the PPP behaves as a glassy polymer. There is a well-defined peak in the stress–strain curve at approximately 3% strain, which represented material yielding. After softening to approximately 35 MPa, the stress remained relatively stable up to approximately 20% strain. Beyond this point, the stress increased steadily with strain until near failure. For all samples tested, the average yield stress was approximately 50 MPa, the average failure stress was approximately 49 MPa, and the average strain-to-failure was approximately 75%. Increasing temperature to 175°C, the PPP was measured to be weaker, less tough, and more compliant; although the strain-to-failure was greater. The average strength is approximately 12 MPa, and the average strain-to-failure is approximately 144%. The yield-stress peak in the stress–strain curve observed at 155°C was no longer present at 175°C. Accordingly, the samples tested at 195°C and 210°C had comparably low strengths and moduli, and very high strains-to-failure. Their average strengths were approximately 1.5 MPa and 0.67 MPa, respectively. Their average strains-to-failure values were 553% and 296%, respectively. It should be noted that these

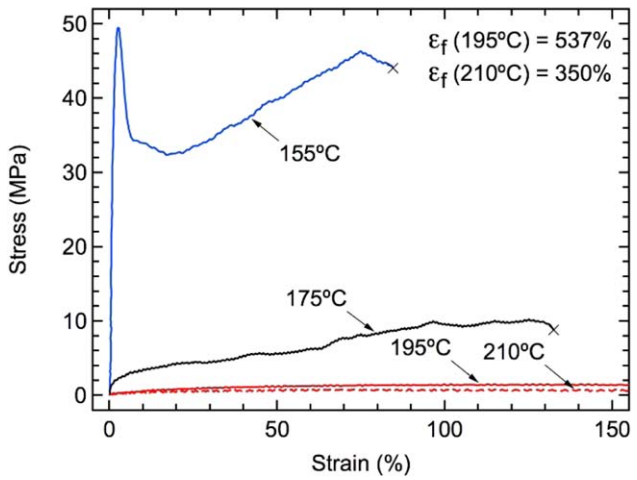

Figure 4. Stress–strain behavior for representative PPP specimens at temperatures ranging between 155°C and 210°C. [Color figure can be viewed in the online issue, which is available at wileyonlinelibrary.com.]

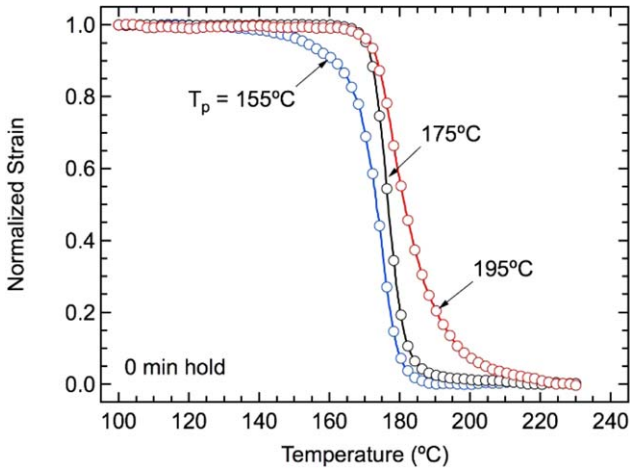

Figure 5. Normalized shape-recovery plots of representative PPP samples programmed at 155°C, 175°C, and 195°C. These samples were cooled immediately upon reaching 50% strain. All samples showed complete or nearly complete shape recovery. [Color figure can be viewed in the online issue, which is available at wileyonlinelibrary.com.]

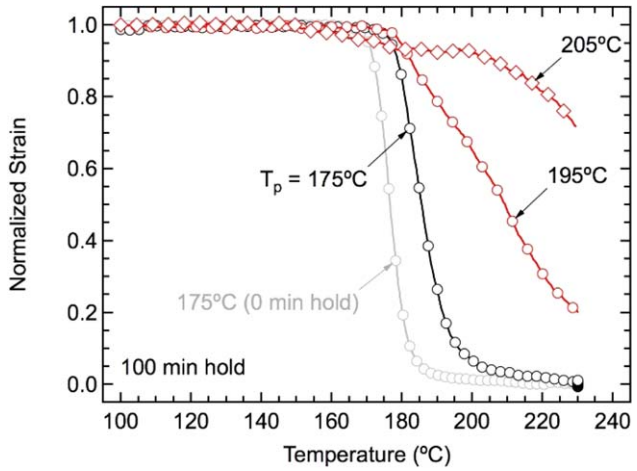

Figure 6. Normalized shape-recovery plots of representative PPP samples programmed to 50% strain at 175°C, 195°C, and 205°C and then allowed to relax for 100 min. Only specimens programmed at 175°C showed full recovery. [Color figure can be viewed in the online issue, which is available at wileyonlinelibrary.com.]

samples did not rupture the same way the 155°C and 175°C samples did, but rather pinched apart at the failure point.

Shape-Memory Recovery

Representative recovery curves for free-recovery samples programmed at 155°C, 175°C, and 195°C are shown in Figure 5. The rationale for the programming temperatures chosen was to evaluate the effects by programming (1) below the glass transition, (2) within the glass transition, and (3) above the glass transition but below melting and flow. In these tests, the samples were quenched immediately to 100°C after the desired programmed strain level was reached, wherein the quenching process took less than 3 min. The fixity values for all samples programmed ranged between 97% and 98%, demonstrating excellent shape fixing of the samples. During recovery, the initiation temperature (T_i) was measured to be 166°C, for the samples deformed at 155°C, although a small amount of recovery was induced as low as 125°C. For samples programmed at 175°C and 195°C, the T_i was measured as 173°C. Although the samples programmed at 155°C initiated recovery at a lower temperature, the recovery behavior roughly converged to match that of the samples programmed at 175°C. Conversely, while the samples programmed at 175°C and 195°C initiated at the same temperature, the samples programmed at 195°C diverged, requiring higher temperatures to achieve complete recovery. In all the samples tested, normalized strain recovery ranged between 99% and 100% (i.e., nearly all the applied strain was recovered); however, the samples programmed at 175°C showed more ideal shape-recovery behavior (e.g., sharper transitions more closely resembling a step function).

The effect of relaxation during programming on the shape-memory recovery was also evaluated. PPP samples were deformed at 175°C, 195°C, and 205°C and allowed to relax for 100 min before cooling (Figure 6). For the samples deformed at 175°C and 195°C and held for 100 min, the T_i was approximately 178°C and 179°C, respectively, higher than their immediately cooled counterparts. In general, their recovery profiles were shifted to higher temperatures relative to their immediately cooled counterparts. The rate of recovery, measured as the slope when half the stored strain was recovered, also decreased for the samples allowed to relax during programming. The rate of recovery decreased from 6%/°C to 3.3%/°C for samples programmed at 175°C, and decreased from 3%/°C to 1.1%/°C for samples programmed at 195°C. The T_i of the 205°C sample could not be calculated because the 205°C sample did not recover at least half of its programmed strain, although visually it was estimated to occur above 200°C. The final recovery fraction was approximately 100%, 80%, and 28% for the samples deformed and relaxed at 175°C, 195°C, and 205°C, respectively. The addition of relaxation time to the programming method appears to have a much more pronounced effect on the recovery behavior of the material than changes in temperature alone.

In addition to free-recovery tests, partially-constrained recovery tests were also performed. For many real-world shape memory applications the material must recover against a bias force, so quantifying the constrained-recovery behavior is an important step in determining the efficacy of the material in shape-memory applications. Based on the previous results, samples were deformed at 175°C and quenched immediately. Figure 7(a) features representative recovery curves for the partially-constrained recovery tests. Specimens initiated recovery at temperatures between 170°C and 175°C, consistent with that observed in Figure 5. Samples reached a strain recovery maximum (i.e., a minimum point on the curve), and then dramatically increased in strain with increasing temperature due to the bias stress applied. The maximum amount of strain recovered was inversely related to constraint; e.g., for a bias stress of 0 MPa full recovery was observed, and for a bias stress of 8.9 MPa no recovery was observed. This is highlighted in Figure 7(b), which explicitly shows the fraction of deformation recovered as a function of constraining stress. The graph illustrates an exponentially-shaped decaying relationship between recovery and constraining stress.

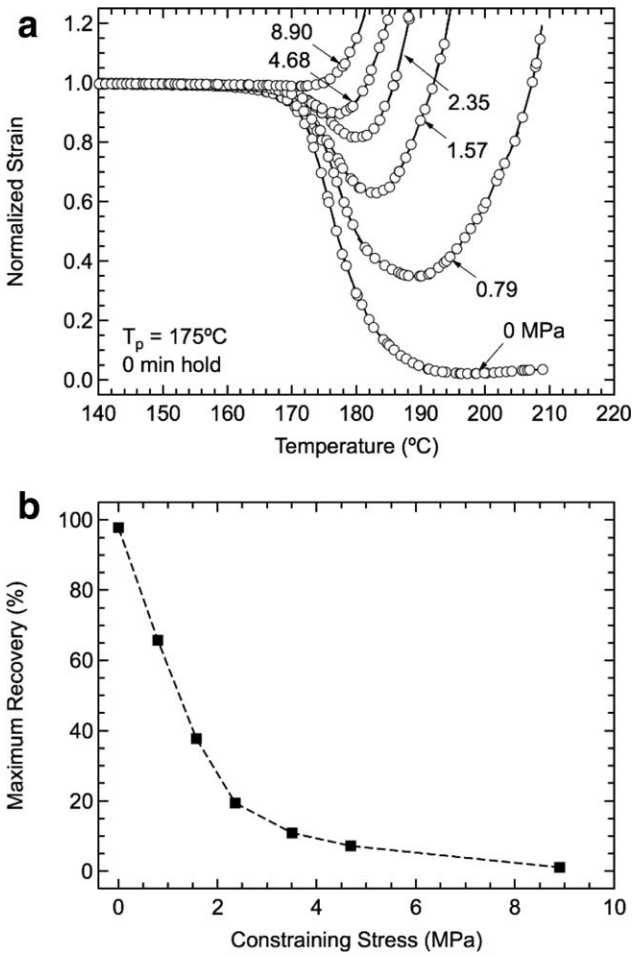

Figure 7. (a) Normalized constrained-recovery curves for representative PPP specimens. (b) Maximum recovered strain fraction of PPP as a function of constraining load. Bias stress ranged from 0 MPa to 8.9 MPa.

Furthermore, the temperature of maximum recovery scaled inversely with bias stress as well [Figure 7(a)].

DISCUSSION

In order for a polymer to demonstrate shape-memory properties, the microstructure of the material must have two features: (1) a form of crosslinking or "hard points" in the microstructure, which controls the memorized shape of the material, and (2) a reversible phase transition, which can lock the programmed shape until recovery is induced.[25] However, for a material to function as an effective SMP, additional conditions must be satisfied. The transition of the material from programmed to memorized state should occur over a relatively narrow temperature range,[25] and the storage modulus must decrease by at least two decades.[47] This ensures that the material will store the programmed shape well upon cooling and recover quickly upon heating. Lastly, for most applications, a large amount of programmed strain is desired. Therefore, the material must be able to withstand large amounts of deformation.

The purpose of this study was to evaluate the behavior of PPP as a high-strength SMP, and to establish a link between time–temperature superposition and shape-memory behavior. Previous studies have shown encouraging results with other aromatic polymers[27,29,30] that demonstrated reasonable shape fixity and deformation recovery. As shown in Figure 5 for temperatures in-and-around the glass transition, PPP exhibited good shape recovery if deformed and cooled relatively quickly. Furthermore, the specific deformation temperatures tested did not have a large effect on the shape recovery. However, the combination of long deformation times and high temperatures lead to poor shape recovery, illustrated in Figure 6. This overall behavior can perhaps be best understood through careful observation of the relaxation modulus master curve relative to shape-recovery behavior shown in Figure 3(b). Recall that each component curve corresponded to an isothermal temperature, and these component curves were shifted into a continuous master curve, quantified by eqs. (1) and (2) and the WLF constants shown in Table I. Programming of an SMP is analogous to the experimental conditions of creating a relaxation modulus master curve, in the respect that both involve straining the material at a temperature within the glass transition in which relaxation can occur. It is our belief that the programming temperature and hold time can be used to derive an equivalent hold time on the master curve to predict the amount of relaxation and explain shape-memory behavior. Utilizing this approach, it is possible to derive the hold time necessary to reach a prescribed relaxation modulus for any given temperature and avoid loss of shape memory. For example, Figure 8(a) shows the relaxation master curve, highlighting the equivalent relaxation time for specimens deformed and held at 175°C for 200 min, 185°C for 8.5 min, and 195°C for 1.4 min, resulting in a nearly equivalent relaxation modulus of approximately 2.5 MPa at 510 sec. In this illustration, the starting points for each condition correspond to the storage modulus at the specified programming temperature. Correspondingly, these three combinations showed nearly identical shape-recovery behavior shown in Figure 8(b). These relaxation times were chosen specifically because they lie in the rubbery regime of the relaxation modulus. Conversely, for increased temperatures with longer hold times, such as the 205°C held for 100 min, the equivalent relaxation time was 20,000 sec and corresponds to when the sample has entered the flow regime. This behavior can be associated with poor shape recovery as shown in Figure 6, in which samples do not fully recover to their original shape. Therefore, Figure 8 demonstrates that the shape-memory behavior of PPP is highly dependent on the TTS behavior. With increasing temperature or increasing hold time, time-dependent visco-elastic/plastic effects on molecular motion are allowed to activate, causing permanent deformation, which severely hinder shape memory. If the PPP is deformed at 195°C or 205°C and allowed to relax for 100 min, the material will be well within its flow regime. However, if the material is programmed at 175°C and allowed to relax for 100 min, the final relaxation modulus was still in the rubbery regime, where deformation is recoverable. As the relaxation modulus is a macroscopic measurement of this chain motion, it is logical that the recovery behavior of the material can be directly linked to this viscoelastic property.

As mentioned previously, the shift factors and therefore the WLF constants should be the same for all viscoelastic properties.[48]

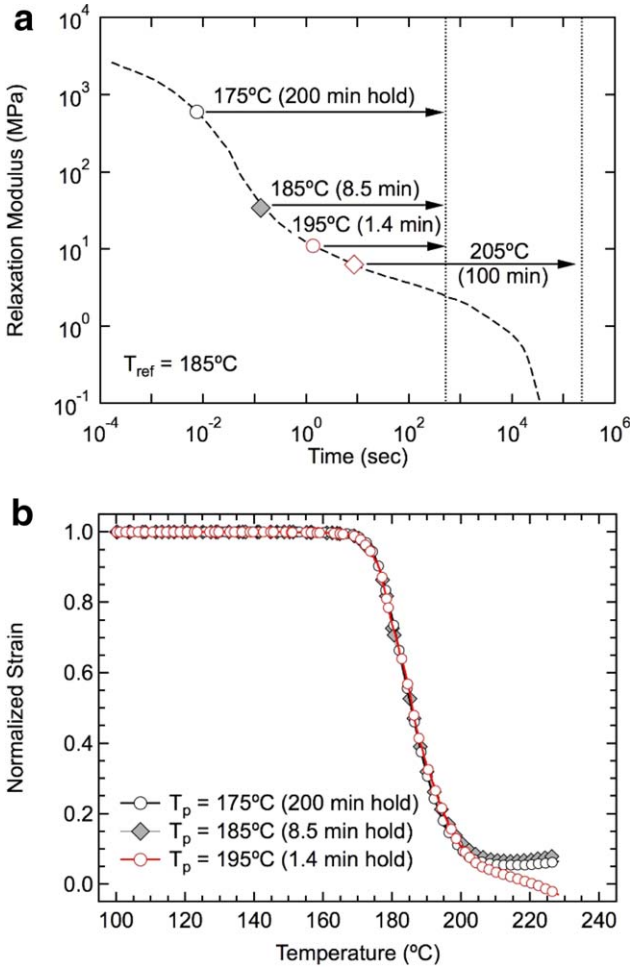

Figure 8. (a) Relaxation master curve, illustrating relaxation modulus as a function of hold time for various temperatures and (b) corresponding shape-recovery behavior. [Color figure can be viewed in the online issue, which is available at wileyonlinelibrary.com.]

As shown in Table I, the WLF constants were found to be very similar between the storage and relaxation modulus master curves. Aside from statistical variations in the mechanical properties of polymers, most of the disparities between these values are likely related to the time scales of the tests. To construct the relaxation modulus master curves, the samples were relaxed for 20 min at each temperature. By contrast, the longest time scale of the storage modulus master curve tests was approximately 2.2 sec. Significantly, more molecular motion is likely over the longer time scale tests, which may be the source of the discrepancy between the WLF constants for the two different viscoelastic functions.

The results shown in Figure 7 illustrate the shape-memory response of PPP under load-constrained conditions. Predictably, the amount of recoverable deformation scaled inversely with bias force; however, Figure 7(b) shows an exponentially decaying relationship, rather than a linear one observed in previous shape-memory investigation.[49] The difference in shape is likely due to the nature of the materials investigated; the PPP used in this study is a thermoplastic, while Lakhera *et al.* utilized crosslinked methacrylate networks. Therefore, at temperatures near the glass transition, time dependent processes are expected to be more significant for thermoplastic PPP. This is exemplified by the dramatic increase in strain with increasing temperature observed in PPP [Figure 7(a)], illustrating the permanent deformation induced by the bias stress. Conversely, the crosslinked networks tested by Lakhera *et al.* reached a stable plateau at elevated temperatures in the rubbery regime.

This study introduces the use of thermoplastic PPP as a potential high-strength SMP material. These results demonstrate that TTS can be used to understand the effects of programming time and temperature on this material. It should be noted that TTS is often used in the thermoviscoelastic modeling of thermoset SMPs.[50–54] In general, these studies utilize models consisting of thermal components (typically Kelvin-Voigt models) and mechanical components (typically a spring in parallel with one or more Maxwell elements). These models do an excellent job in predicting the effects of structural relaxation (physical ageing) and stress relaxation during programming, storage, and recovery. However, it is important to remember that they do not capture visco-plastic behavior experienced in thermoplastics; in this sense, this study is the first to propose using TTS to explain and predict the influence of programming on free-recovery behavior in thermoplastic SMPs. Our results suggest that by keeping an equivalent relaxation time within the rubbery regime of the relaxation modulus master curve, the loss of entanglements (e.g. physical crosslinks) will be avoided, and the material will be able to maintain full shape recovery under unconstrained conditions. To illustrate this effect in a practical application, we demonstrated this in a relatively thick-walled heat-shrink PPP tube (Figure 9). In this demonstration, PPP tubes were expanded to a maximum inner diameter of 13 mm at 175°C within 10 min. This corresponds to approximately 30 sec of relaxation time at 185°C, well within the rubbery modulus of the relaxation master curve. Following the programming step, it was found that the tubes showed 99.7% fixity after unloading with a final programmed diameter of 12.96 mm. Using the change in inner diameter as a first order approximation, a stored strain of approximately 62% was calculated. However, it is acknowledged that the local strain state is more complicated, as evidenced by the permanent longitudinal lines imprinted by the steel pin actuators. Following recovery at 200°C, the percent recovery of the inner diameter was found to

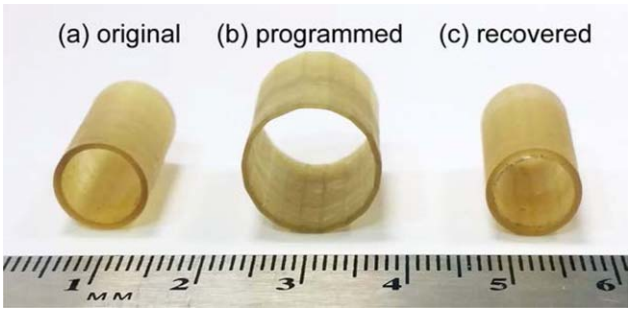

Figure 9. (a) A hollow PPP tube was manufactured and (b) programmed to 62% circumferential strain at 175°C within 10 min. (c) The PPP tube demonstrated complete shape recovery when reheated to 200°C. [Color figure can be viewed in the online issue, which is available at wileyonlinelibrary.com.]

be 96.3% with a final recovered diameter of 8.18 mm. While the PPP material may experience permanent deformation under a constant load at high temperatures, this application would still be able to provide structural support at temperatures below 150°C due to the inherently high mechanical properties of PPP.

CONCLUSIONS

The shape-memory behavior of thermoplastic PPP was investigated as a function of programming temperatures, relaxation times, and recovery conditions. The relaxation modulus master curve was created using time–temperature superposition to explain the influence of programming conditions on free-recovery behavior. From this study, the following conclusions were found:

1. PPP was able to demonstrate high shape fixity (over 97%) for all conditions tested in this study. The material was also capable of complete free-recovery if programmed between 155°C and 195°C with no relaxation before cooling and storage.
2. During programming, extended relaxation times at elevated temperatures decreased the ability of PPP to act as a shape-memory polymer. The total amount of free-recovery decreased as the equivalent relaxation time corresponded to the melt/flow regime of the relaxation modulus master curve.
3. Under constrained-recovery conditions, the maximum recoverable deformation scales with an exponentially decreasing relationship to bias force. If a bias force is applied, shape recovery will be lost with continued heating past T_g.
4. The shape-memory effect in PPP has potential for various applications as demonstrated by the heat shrink tubing. The PPP tubing was programmed at 175°C within 10 min and was able to recover 96% of the programmed strain (62%).

ACKNOWLEDGMENTS

CPF and CMY gratefully acknowledge support from Solvay Specialty Polymers, LLC. DAC thanks the University of Wyoming Energy Graduate Assistantship program for support. The authors would like to thank Ellana Taylor for her help in the preparation and characterization of PPP samples.

REFERENCES

1. Ratna, D.; Karger-Kocsis, J. *J. Mater. Sci.* **2008**, *43*, 254.
2. Mather, P. T.; Luo, X. F.; Rousseau, I. A. *Annu. Rev. Mater. Res.* **2009**, *39*, 445.
3. Rousseau, I. A. *Polym. Eng. Sci.* **2008**, *48*, 2075.
4. Hu, J. L.; Zhu, Y.; Huang, H. H.; Lu, J. *Prog. Polym. Sci.* **2012**, *37*, 1720.
5. Leng, J. S.; Lan, X.; Liu, Y. J.; Du, S. Y. *Prog. Mater. Sci.* **2011**, *56*, 1077.
6. Xie, T. *Polymer* **2011**, *52*, 4985.
7. Julich-Gruner, K. K.; Lowenberg, C.; Neffe, A. T.; Behl, M.; Lendlein, A. *Macromol. Chem. Phys.* **2013**, *214*, 527.
8. Berg, G. J.; McBride, M. K.; Wang, C.; Bowman, C. N. *Polymer* **2014**, *55*, 5849.
9. Peponi, L.; Navarro-Baena, I.; Kenny, J. M. In Smart Polymers and Their Applications; Aguilar, M. R.; SanRoman, J., Eds.; Woodhead Publishing: Cambridge, **2014**; p 204.
10. Behl, M.; Lendlein, A. *Mater. Today* **2007**, *10*, 20.
11. Yakacki, C. M.; Gall, K. In Shape-Memory Polymers; Springer-Verlag Berlin: Berlin, **2010**; p 147.
12. Rodriguez, J. N.; Miller, M. W.; Boyle, A.; Horn, J.; Yang, C. K.; Wilson, T. S.; Ortega, J. M.; Small, W.; Nash, L.; Skoog, H.; Maitland, D. J. *J. Mech. Behav. Biomed. Mater.* **2014**, *40*, 102.
13. Small, W.; Buckley, P. R.; Wilson, T. S.; Benett, W. J.; Hartman, J.; Saloner, D.; Maitland, D. J. *IEEE Trans. Biomed. Eng.* **2007**, *54*, 1157.
14. Ware, T.; Simon, D.; Hearon, K.; Liu, C.; Shah, S.; Reeder, J.; Khodaparast, N.; Kilgard, M. P.; Maitland, D. J.; Rennaker, R. L.; Voit, W. E. *Macromol. Mater. Eng.* **2012**, *297*, 1193.
15. Nash, L. D.; Wierzbicki, M. A; Maitland, D. J. Design Characterization, *J. Med. Dev. Trans. ASME* **2014**, *8*, 020911.
16. Yu, K.; Ritchie, A.; Mao, Y.; Dunn, M. L.; Qi, H. J. *Procedia IUTAM* **2015**, *12*, 193.
17. Ge, Q.; Qi, H. J.; Dunn, M. L. *Appl. Phys. Lett.* **2013**, *103*, 131901.
18. Yakacki, C. M.; Nguyen, T. D.; Likos, R.; Lamell, R.; Guigou, D.; Gall, K. *Polymer* **2011**, *52*, 4947.
19. Qi, H. J.; Nguyen, T. D.; Castro, F.; Yakacki, C. M.; ShandaSa, R. *J. Mech. Phys. Solids* **2008**, *56*, 1730.
20. Jones, D. P.; Leach, D. C.; Moore, D. R. *Polymer* **1985**, *26*, 1385.
21. Brady, D. G. *J. Appl. Polym. Sci.* **1976**, *20*, 2541.
22. Akhtar, S.; White, J. L. *Polym. Eng. Sci.* **1992**, *32*, 690.
23. Trotignon, J. P.; Verdu, J.; Martin, C.; Morel, E. *J. Mater. Sci.* **1993**, *28*, 2207.
24. Abu Bakar, M. S.; Cheng, M. H. W.; Tang, S. M.; Yu, S. C.; Liao, K.; Tan, C. T.; Khor, K. A.; Cheang, P. *Biomaterials* **2003**, *24*, 2245.
25. Liu, C.; Qin, H.; Mather, P. T. *J. Mater. Chem.* **2007**, *17*, 1543.
26. Wang, Q. H.; Bai, Y. K.; Chen, Y.; Ju, J. P.; Zheng, F.; Wang, T. M. *J. Mater. Chem. A* **2015**, *3*, 352.
27. Yoonessi, M.; Shi, Y.; Scheiman, D. A.; Lebron-Colon, M.; Tigelaar, D. M.; Weiss, R. A.; Meador, M. A. *ACS Nano* **2012**, *6*, 7644.
28. Koerner, H.; Strong, R. J.; Smith, M. L.; Wang, D. H.; Tan, L. S.; Lee, K. M.; White, T. J.; Vaia, R. A. *Polymer* **2013**, *54*, 391.
29. Wu, X. L.; Huang, W. M.; Ding, Z.; Tan, H. X.; Yang, W. G.; Sun, K. Y. *J. Appl. Polym. Sci.* **2014**, *131*, 39844.
30. Shi, Y.; Yoonessi, M.; Weiss, R. A. *Macromolecules* **2013**, *46*, 4160.
31. Frick, C. P.; DiRienzo, A. L.; Hoyt, A. J.; Safranski, D. L.; Saed, M.; Losty, E. J.; Yakacki, C. M. *J. Biomed. Mater. Res. Part A* **2014**, *102*, 3122.
32. Friedrich, K.; Burkhart, T.; Almajid, A. A.; Haupert, F. *Int. J. Polym. Mater.* **2010**, *59*, 680.

33. Nunes, J. P.; Silva, J. F.; Velosa, J. C.; Bernardo, C. A.; Marques, A. T. *Plast. Rubber Compos.* **2009**, *38*, 167.
34. Dean, D.; Husband, M.; Trimmer, M. *J. Polym. Sci. B Polym. Phys.* **1998**, *36*, 2971.
35. Ha, Y. H.; Scott, C. E.; Thomas, E. L. *Polymer* **2001**, *42*, 6463.
36. Carter, R.; Wang, J.; Lee, P. C.; Park, C. B. *J. Cell. Plast.* **2005**, *41*, 29.
37. Kimerling, T. E.; Yao, D. G.; Kim, B. H. *Polym. Plast. Technol. Eng.* **2009**, *48*, 1008.
38. Morgan, S. E.; Misra, R.; Jones, P. *Polymer* **2006**, *47*, 2865.
39. Kemmish, D. J.; Hay, J. N. *Polymer* **1985**, *26*, 905.
40. Tregub, A.; Harel, H.; Marom, G.; Migliaresi, C. *Compos. Sci. Technol.* **1993**, *48*, 185.
41. Chivers, R. A.; Moore, D. R. *Polymer* **1994**, *35*, 110.
42. Martin, A. C.; Lakhera, N.; DiRienzo, A. L.; Safranski, D. L.; Schneider, A. S.; Yakacki, C. M.; Frick, C. P. *Compos. Sci. Technol.* **2013**, *89*, 110.
43. Burstone, C. J.; Liebler, S. A. H.; Goldberg, A. J. *Am. J. Orthod. Dentofacial Orthoped.* **2011**, *139*, e391.
44. Pei, X. Q.; Friedrich, K. *Wear* **2012**, *274*, 452.
45. Hoyt, A. J.; Yakacki, C. M.; Fertig, R. S.; Carpenter, R. D.; Frick, C. P. *J. Mech. Behav. Biomed. Mater.* **2015**, *41*, 136.
46. Williams, M. L.; Landel, R. F.; Ferry, J. D. *J. Am. Chem. Soc.* **1955**, *77*, 3701.
47. Ortega, A. M.; Kasprzak, S. E.; Yakacki, C. M.; Diani, J.; Greenberg, A. R.; Gall, K. *J. Appl. Polym. Sci.* **2008**, *110*, 1559.
48. Ferry, J. D. Viscoelastic Properties of Polymers. 3rd ed.; Wiley: New York, **1980**; p 672.
49. Lakhera, N.; Yakacki, C. M.; Nguyen, T. D.; Frick, C. P. *J. Appl. Polym. Sci.* **2012**, *126*, 72.
50. Davidson, J. D.; Goulbourne, N. C. *Smart Mater. Struct.* **2015**, *24*, 055014.
51. Nguyen, T. D.; Yakacki, C. M.; Brahmbhatt, P. D.; Chambers, M. L. *Adv. Mater.* **2010**, *22*, 3411.
52. Xiao, R.; Choi, J. W.; Lakhera, N.; Yakacki, C. M.; Frick, C. P.; Nguyen, T. D. *J. Mech. Phys. Solids* **2013**, *61*, 1612.
53. Ge, Q.; Yu, K.; Ding, Y. F.; Qi, H. J. *Soft Matter* **2012**, *8*, 11098.
54. Li, G. Q.; Xu, W. *J. Mech. Phys. Solids* **2011**, *59*, 1231.